Project 4 - FYS4150

Nanna Bryne, Johan Mylius Kroken, Vetle A. Vikenes
(Dated: November 29, 2022)

We investigate the 2D Ising model on a $(L \times L)$ lattice with beriodic boundary conditions by using the Metropolis algorithm to perform Monte Carlo simulations on the system. By performing Monte Carlo simulations we are able to compute estimates of the thermodynamical properties of the Ising model, in particular the specific heat capacity, C_V, and magnetic susceptibility, χ. We study the temperature dependence of C_V for lattice sizes of $L \in [40, 60, 80, 100]$, from which we are able to estimate the critical temperatures where a phase transition occurs. By combining these results with finite size scaling relations, we are able to obtain an estimated value of the critical temperature for the 2D Ising model of infinite size. We estimate this critical temperature to be $T_C(L = \infty) \approx 2.2651\, J/k_B$, compared to the analytical solution $T_C(L = \infty) \approx 2.2692\, J/k_B$ as found by Lars Onsager in 1944 [2]
Supporting material may be found in the following GitHub repository: https://github.com/Vikenes/FYS4150/tree/main/project4.

I. INTRODUCTION

In his 1944 paper [2], Lars Onsager found an analytical solution to the 2D Ising model. Very briefly, the Ising model is a mathematical model designed to model ferromagnetism in statistical mechanics on a microscopic level. When the 1D model (Ising chain) was introduced, it was quickly discovered that there was no evidence for any phase transition occurring. In two dimensions however, approximate solutions of the Ising model showed indication of phase transitions. The analytical solution of Onsager came around 20 years after the analytical solution of the 1D model. To this day, an analytical solution of the Ising model in three dimensions does not exist. The aim of this investigation is to reproduce, numerically, one of Onsager's results; that of the critical temperature for the 2D Ising model of infinite size.

Measuring this exactly is hard due to the size and properties of statistical ensembles (especially for large grids). However, they may be estimated using stochastic sampling, for example by means of Markov chain Monte Carlo sampling. We will implement this through the Metropolis algorithm and use theoretical properties of phase transition phenomena to numerically investigate and compare our model to the analytical result found by Onsager.

The investigation will be structured as follows: Section II gives a brief introduction to the relevant theoretical background of our methods. Section III outlines how we implement and adapt various aspects of the theory to simulate the Ising model numerically. In section IV we present the different methods we will consider for our analysis. The results are then presented in section V, discussed in section VI, and we make a final conclusion in section VII. Supporting figures, equations and tables that are not directly contributing towards the main analysis are presented as supplementary material in Appendix.

II. THEORETICAL BACKGROUND

In this section we present a brief introduction to the 2D Ising model, as well as some theoretical background of phase transition phenomena and statistical mechanics. Additionally, we briefly describe the overall ideas behind the workings of Markov chain Monte Carlo (MCMC) methods, in particular how this is implemented with the Metropolis algorithm. A more detailed explanation of our implementations will be presented in Sec. III.

A. The 2D Ising model

The Ising model is a mathematical model used to model statistical properties of materials, such as ferromagnetism. It consists of discrete magnetic moments localized in a particular lattice. For simplicity, we will refer to the magnetic moments as "spins" throughout this report. Additionally, we will consider a square lattice of dimension $(L \times L)$, where we refer to L as the lattice size. Each spin has a fixed position in the lattice, where they are allowed to interact with their immediate neighbors. We will denote a single spin as s_i, where the subscript i refers to a certain position in the lattice. An individual spin can be in one of two possible states having a value of $s_i = +1$ or $s_i = -1$. We will refer to an arbitrary spin state of the entire lattice as a *microstate*, which we will denote as ν[1]. The number of individual spins in the lattice is thus $N = L^2$. We will limit our analysis to the case of no external magnetic field. The total energy of the system is given by

$$E(\nu) = -J \sum_{\langle kl \rangle}^{N} s_k s_l, \tag{1}$$

where $\langle kl \rangle$ indicates that the sum is taken over the nearest neighboring pairs of spins. We will in this report

[1] In practice, ν can thus be viewed as an $L \times L$ matrix.

impose periodic boundary conditions, so all spins have exactly four neighbors (left, right, up and down). The parameter J represents the strength of interactions between neighboring spins, and we assume a constant $J > 0$, so that the energy is lower when neighboring spins are aligned.

The total magnetization of the system will be given by the sum over all spins

$$M(\nu) = \sum_i^N s_i. \tag{2}$$

B. Statistical mechanics

The probability of the system being in a microstate ν at a given energy and a constant temperature, T, is governed by the Boltzmann distribution

$$p_\nu(T) = \frac{1}{Z} e^{-\beta E(\nu)}, \tag{3}$$

where $\beta = 1/k_B T$ with k_B being the Boltzmann constant. Z is the partition function, defined as

$$Z = \sum_\nu e^{-\beta E(\nu)}, \tag{4}$$

where the sum goes over all possible microstates ν.

For an observable $Q(\nu)$, its expectation value is given by

$$\langle Q \rangle = \sum_\nu Q(\nu)\, p_\nu(T) = \frac{1}{Z} \sum_\nu Q(\nu) e^{-\beta E(\nu)}. \tag{5}$$

These averages will eventually converge towards their true thermal averages[3, p. 247]. Two quantities we will focus on in this report are the specific heat capacity, C_V, and the magnetic susceptibility, χ, both normalized to the number of spins, N, which are defined as

$$C_V = \frac{1}{N} \frac{1}{k_B T^2} \left(\langle E^2 \rangle - \langle E \rangle^2 \right), \tag{6}$$

$$\chi = \frac{1}{N} \frac{1}{k_B T} \left(\langle M^2 \rangle - \langle |M| \rangle^2 \right), \tag{7}$$

where the various average quantities are obtained from Eq. (5). We will later be concerned with the energy and magnetization of our system per spin, which we define as

$$\epsilon(\nu) = \frac{E(\nu)}{N}, \tag{8}$$

$$m(\nu) = \frac{M(\nu)}{N}. \tag{9}$$

C. Phase transitions and critical phenomena

One of the most peculiar features of continuous phase transitions is that thermodynamic quantities are found to exhibit similar behavior for a variety of different systems. These phase transitions can be characterized by *critical exponents*, where physical quantities behave according to power laws near the critical point, i.e. a critical temperature. Near the critical temperature, $\langle |M| \rangle$, C_V and χ behave according to the following power laws:

$$\langle |M| \rangle \propto |T - T_c(L = \infty)|^\beta, \tag{10}$$

$$C_V \propto |T - T_c(L = \infty)|^{-\alpha}, \tag{11}$$

$$\chi \propto |T - T_c(L = \infty)|^{-\gamma}, \tag{12}$$

where the critical exponents of the 2D Ising model we consider are $\beta = 1/8$[2], $\alpha = 0$ and $\gamma = 7/4$ [4]. Both C_V and χ will therefore diverge near the critical temperature[3]. $T_c(L = \infty)$ is the critical temperature according to a square lattice Ising model of infinite size. Additionally, the correlation between spins is characterized by the correlation length, ξ, which has the following power law behavior near the critical temperature

$$\xi \propto |T - T_c(L = \infty)|^{-\nu}, \tag{13}$$

where $\nu = 1$[4]. Our analysis is limited to systems of finite extent, and it can be shown that the correlation length is proportional to the lattice size near the critical temperature[1]. For $T = T_c(L)$, we then have $\xi \propto L$. Inserting this into Eq. (13), we get a relation between the lattice size L and the associated critical temperature, $T_c(L)$

$$T_c(L) - T_c(L = \infty) = aL^{-1}, \tag{14}$$

where a is a proportionality constant. By estimating the critical temperature at different lattice sizes, we can perform linear regression to obtain an estimate of $T_c(L = \infty)$. This estimate can be compared to the analytical value of $T_c(L = \infty)$, which for the 2D Ising model with no external magnetic field is [2]

$$T_c(L = \infty) = \frac{2}{\ln(1 + \sqrt{2})} J/k_B \approx 2.2692\, J/k_B. \tag{15}$$

D. Monte Carlo methods

To study thermodynamic properties of the Ising model, we need to compute the partition function in Eq. (4). However, this would require a sum over all possible microstates. For a lattice of size L the total number of unique microstates is $2^{L^2} = 2^N$. This become an impossible task for the lattice sizes we are going to consider.

---

[2] The exponent β is not to be confused with the inverse temperature.

[3] A critical exponent of $\alpha = 0$ means that C_V diverges logarithmically.

[4] Not to be confused with the microstate, ν.

To overcome this problem we may draw random samples of the system and use these samples to estimate thermal averages. A common choice for sampling the system is the Markov chain Monte Carlo (MCMC) method. A Markov chain is a stochastic process in which the outcome of an event is independent of the process's history. Loosely speaking, it can be regarded as a random walk in state space. There are several algorithms for constructing these Markov chains, but the one we will consider is a variant of the *Metropolis-Hastings* algorithm.

E. Metropolis algorithm

The Metropolis algorithm uses a Markov process to generate multiple samples of microstates that approximate a Boltzmann weighted ensemble. A Markov process is defined by a transition probability, $W(\nu \to \nu')$, which is the probability of the system to transition from a state ν to any given state ν'. For the Markov chain to reach the desired distribution we have to fulfill two conditions. The first condition is *ergodicity*, which states that the system has a non-zero probability of going from any state to any other state with a finite sequence of transitions. The second condition is *detailed balance*, meaning that we require each transition to be reversible. That is, the probability for the system to be in a state ν and transition to a state ν' is equal to the probability for the system to be in state ν' and transition to state ν. Mathematically, this can be formulated as

$$P(\nu)W(\nu \to \nu') = P(\nu')W(\nu' \to \nu), \tag{16}$$

where $P(\nu)$ is the distribution of the Markov process. It can be shown that when the conditions of ergodicity and detailed balance are fulfilled, the distribution $P(\nu)$ is both unique and stationary.

A naive approach for sampling configurations would be to sample random microstates uniformly. This has the disadvantage of including microstates which the system is unlikely to be in, and many computations would be required to get a satisfying distribution. Instead, the Metropolis algorithm works by choosing the Boltzmann distribution to sample spins, i.e. $P(\nu) = p_\nu(T)$. If we insert this into Eq. (16) and rewrite it, we get

$$\frac{W(\nu \to \nu')}{W(\nu' \to \nu)} = \frac{p_{\nu'}(T)}{p_\nu(T)} = e^{-\beta \Delta E}, \tag{17}$$

where we defined $\Delta E \equiv E(\nu') - E(\nu)$. Importantly, in Eq. (17) we now see that the partition function has vanished. In general, $W(\nu \to \nu')$ is unknown, and the Metropolis algorithm works by assuming that it can be written as the product of the two probabilities $A(\nu \to \nu')$ and $T(\nu \to \nu')$, the probability of accepting the transition from $\nu \to \nu'$ and the probability of making the transition to ν' being in state ν. One common choice is to assume a symmetric transition probability $T(\nu \to \nu') = T(\nu' \to \nu)$. Eq. (17) then reads

$$\frac{A(\nu \to \nu')}{A(\nu' \to \nu)} = e^{-\beta \Delta E}. \tag{18}$$

Since energy tends to be minimized, a natural choice is to always accept new states if it has a lower energy than the initial state since $\Delta E < 0$ corresponds to transitioning to a state with a higher probability. Assuming an acceptance probability of 1 for a transition resulting in a lower energy, we can express the transition probability $A(\nu \to \nu')$ as

$$A(\nu \to \nu') = \min\left(1, e^{-\beta \Delta E}\right). \tag{19}$$

With Eq. (19), we will always transition to states with lower energies. Since ergodicity must be fulfilled, we may not reject any transition that doesn't lower the energy. In Sec. III B we discuss how we implement this in practice.

III. IMPLEMENTATIONS

For our computations we will use J and J/k_B as the base units for energy and temperature, respectively.

A. Energy change due to single spin flip

When flipping a single spin there is a limited number of possible values ΔE can take. Consider an arbitrary spin, s_k, in a lattice with $L > 2$. The energy contribution from this spin's interaction with its neighbors is

$$E(s_k) = -J s_k \sum_{\langle l \rangle} s_l. \tag{20}$$

Flipping this spin corresponds to $s_k \to -s_k$. The change in energy from this is $\Delta E = E(-s_k) - E(s_k)$, resulting in the following expression:

$$\begin{aligned} \Delta E &= -J(-s_k) \sum_{\langle l \rangle} s_l - (-J s_k) \sum_{\langle l \rangle} s_l \\ &= 2J s_k \sum_{\langle l \rangle} s_l. \end{aligned} \tag{21}$$

Since each of the spins s_l takes a value of -1 or $+1$, taking the sum over four spins can only yield a value of $\sum_{\langle l \rangle} s_l = \{-4, -2, 0, 2, 4\}$. With $s_k = \pm 1$, it's evident that flipping a single spin results in five possible values of ΔE, which are

$$\Delta E = \{-8, -4, 0, 4, 8\}\, J. \tag{22}$$

Flipping a single spin also yields a change in magnetization, $\Delta M \equiv M(\nu') - M(\nu)$, from the transition

$s_k \to s'_k = -s_k$. The new magnetization due to this transition is easily seen to be $M(\nu') = M(\nu) + 2s'_k$, where the possible values of ΔM are

$$\Delta M = \{-2, +2\}, \tag{23}$$

corresponding to initial spin values of $s_k = \{+1, -1\}$, respectively.

Eqs. (22) and (23) allow for increased efficiency in our numerical implementation of the Metropolis algorithm, which we will discuss in the following section.

B. Metropolis algorithm

To implement the Metropolis algorithm we determine whether to accept a spin flip by comparing $A(\nu \to \nu')$ from Eq. (19) with a random number $r \sim \mathcal{U}(0, 1)$. This method guarantees that the proposed spin flip is accepted if $\Delta E < 0$. Additionally, transitions yielding $\Delta E > 0$ have a higher probability of being accepted if the associated reduction of the Boltzmann distribution is small.

To sample spins, we will draw spins in the lattice according to a uniform random distribution. Below, we present a simple outline of the Metropolis algorithm we use to sample spins.

1. Pick a random spin in the lattice, s_k.
2. Compute resulting ΔE if spin is flipped, according to Eq. (21).
3. If $\exp(-\beta\Delta E) \geq r$: Accept flip,
   $s_k \to -s_k$,
   $E \to E + \Delta E$,
   $M \to M + \Delta M$.
4. If $\exp(-\beta\Delta E) < r$: Reject flip.
5. Repeat.

Repeating this process $N = L^2$ number of times constitutes one MC *cycle*. Using Eq. (22), we compute the five possible values of $\exp(-\beta\Delta E)$ before we begin flipping the spins, rather than evaluating the exponential factor for each spin flip we consider. After one cycle is completed, we store the final energy and magnetization of our lattice, given as one sample. The average energy and magnetization of the lattice are thus obtained by summing up the energy and magnetization from each cycle, and divide by the number of cycles we have run, which we denote as N_{MC}.

C. Parallelization

When we are going to investigate phase transitions, we will have to run MC simulations for multiple temperature values. In order to speed up the process, we will in that case resort to parallelization, where we use the `OpenMP` parallelization method. We have the freedom to implement parallelization at different levels in our simulations, but the one we will consider is to parallelize the temperature iterations, meaning that individual threads are used to run MC simulations at one temperature simultaneously. We provide an example with timed runs with and without parallelization in appendix B, where it becomes evident why this is beneficial.

IV. METHODS

A. Analytical comparison

To test our implementation, we will first consider a lattice of size $L = 2$ for which we can compute the analytical solution. The quantities we will consider are $\langle\epsilon\rangle, \langle|m|\rangle, C_V$ and χ. The analytical derivation of these quantities for $L = 2$ is given in Appendix A. We will estimate the average values numerically for $N_{\text{MC}} = 10^2, 10^3, 10^4, 10^5$, and compare them to the analytical results.

B. Equilibration time

When initializing the system it is unlikely to be in a state near equilibrium. This means that a majority of the cycles we run in the beginning will consist of transitions such that the system approaches an equilibrium. After a certain number of iterations the samples we draw are likely to oscillate around the equilibrium values. The number of cycles needed to reach this equilibrium is called the *equilibration time*. For the sake of consistency however, we will denote it with N_{eq}, to emphasize that we're referring to a number of MC cycles. To reduce the total number of cycles needed to obtain accurate estimates of thermal averages, we only include samples drawn after we have performed N_{eq} cycles initially.

To determine a reasonable choice for N_{eq}, we will consider a lattice with $L = 20$, and plot $\langle\epsilon\rangle$ and $\langle|m|\rangle$ as a function of cycles. We will do this for $T = 1\, J/k_B$ and $T = 2.4\, J/k_B$. For both temperatures, we study the result from a lattice with an ordered initialization (all spins pointing up) and a lattice with an unordered initialization (spins aligned with a uniform random distribution). Based on these plots, we estimate a reasonable choice for N_{eq} by roughly considering the number of N_{MC} required for the estimated averages to stabilize. The value of N_{eq} we obtain from this analysis is the value we will choose for further analysis, unless stated otherwise. When we later refer to sampling the system, all discussions will concern drawing samples after we have equilibrated the system.

C. Estimating the probability distribution

Next, we wish to estimate the probability distribution of the energy, $p_\epsilon(T)$, for a lattice with $L = 20$. To do this, we sample ϵ from a total of $N_{\text{MC}} = 10^5$ subsequent cycles, for $T = 1\,J/k_B$ and $T = 2.4\,J/k_B$. From Eq. (22) we know that the smallest change in ϵ with $N = 400$ spins is $\min(\Delta\epsilon) = 0.01\,\text{J}$. We estimate the probability distributions for the two energies by creating normalized histograms, using $\epsilon = 0.01\,J$ for the bin width. For both temperatures, we also estimate the mean and variance of the distributions.

D. Phase transitions

To estimate the critical temperature for the 2D Ising model of finite extent, $T_c(L)$, we will first study the temperature behavior of C_V and χ for systems of different sizes. From Eq. (15) we know the analytical critical temperature in terms of an infinite sized lattice. To estimate the critical temperature of finite sized lattices, we begin by computing C_V and χ for fifty equally spaced values of $T \in [2,\, 2.5]\,J/k_B$, corresponding to $\Delta T = 0.01\,J/k_B$. We do this for lattices of size $L \in \{40, 60, 80, 100\}$, using $N_{\text{cycles}} = 10^5$ cycles at each temperature for all lattice sizes. According to Eqs. (11) and (12), we expect a diverging behavior of C_V and χ near the critical temperatures. From our initial result, we get a rough estimate of the temperature range in which phase transition occurs, by seeing where C_V and χ exhibit diverging behavior. We then proceed by computing C_V and χ for 100 temperatures in range near the critical temperature. We will then increase the number of cycles by a factor of 10 in order to suppress large variations between subsequent temperature steps.

The critical temperature, or the point of convergence is found by interpolating the values found for C_V and find the temperature for which the interpolated function has a maximum point.

From our estimated values of $T_c(L)$, we can use Eq. (14), and plot the four values of $T_c(L)$ as a function of L^{-1}. From this, we can perform linear regression, and obtain an estimate of $T_c(L = \infty)$ from the intercept of our linear regression.

V. RESULTS

A. Analytical comparison

The comparison between the numerical and analytical values of various quantities is given in table I. The first column shows the total number of cycles run for each of the measured quantities, i.e. these results are obtained *without* equilibrating the system first. Here, we see that we get reasonable good estimates of the average quantities, even for $N_{\text{MC}} = 10^2$. For $nmc = 10^4$ and 10^5 we obtain reasonable approximation of the estimates. However, some fluctuations are to be expected since these are after all numerical approximations.

N_{MC}	$\langle\epsilon\rangle$	$\langle\lvert m\rvert\rangle$	C_V	χ
10^2	-2.0000	1.0000	0.0000	0.0000
10^3	-1.9940	0.9985	0.0479	0.0030
10^4	-1.9960	0.9988	0.0319	0.0035
10^5	-1.9965	0.9988	0.0281	0.0036
Analytical	-1.9960	0.9987	0.0321	0.0040

TABLE I. Comparison of analytical results.

B. Equilibration time

Figure 1 and 2 shows the evolution of $\langle\epsilon\rangle$ for an ordered and unordered initial lattice configuration. A logarithmic scale is used on the x-axis. The result for $T = 1\,J/k_B$ and $T = 2.4\,J/k_B$ are shown in the left and right panel, respectively. For $T = 1\,J/k_B$ we see that an ordered initial configuration quickly approaches the equilibrium value, as aligned spins are favored at low temperature. We see that $N_{\text{MC}} > 10^3$ is required for the unordered configuration to reach close to the equilibrium value. For $T = 2.4\,J/k_B$ we see that both lattice configurations require an approximate value of 10^4 cycles in order to equilibrate the system, as higher temperatures favor less alignment of spins. The evolution of $\langle\lvert m\rvert\rangle$ in Fig. 2

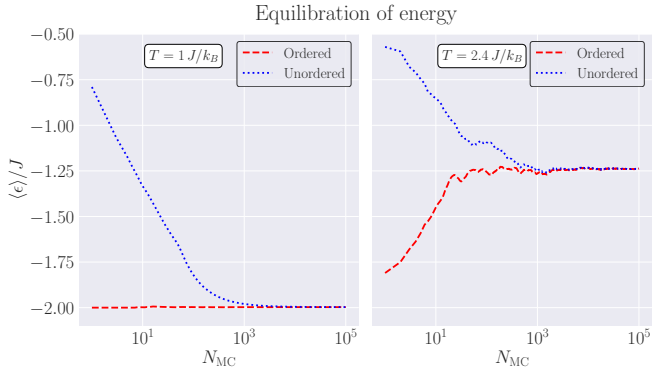

FIG. 1. Equilibration time for the mean energy $\langle\epsilon\rangle$ as function of the number of Monte Carlo cycles, N_{MC}, for $T = 1\,J/k_B$ and $T = 2.4\,J/k_B$. The red line correspond to an ordered initial state in which all the spins point in the same direction. The blue line correspond to an unordered initial state with random initialization of the spins.

shows a similar behavior to that of $\langle\epsilon\rangle$ in Fig. 1. An ordered lattice configuration reaches the equilibrium values after very few iterations for $T = 1\,J/k_B$, compared to the unordered configuration. At $T = 2.4\,J/k_B$ both configurations require $N_{\text{MC}} \approx 10^4$ for equilibrium to be reached.

Based on these plots we choose $N_{\text{eq}} = 1.5 \cdot 10^4$ for further analysis. In Figs. 1 and 2 we saw that an approximate equilibrium was reached after 10^4 cycles. There are statistical uncertainties in our results due to considering one sample only, and we therefore choose the slightly higher value of $N_{\text{eq}} = 1.5 \cdot 10^4$. This value is also small enough for the simulations to be computationally efficient.

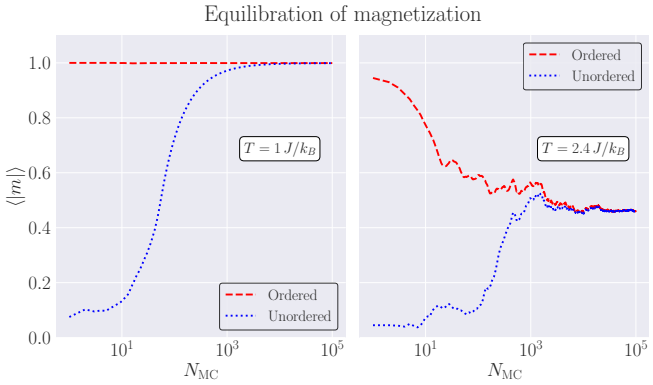

FIG. 2. Equilibration time for the mean magnetization $\langle |m| \rangle$ as function of the number of Monte Carlo cycles, N_{MC}, for $T = 1\, J/k_B$ and $T = 2.4\, J/k_B$. The red line correspond to an ordered initial state in which all the spins point in the same direction. The blue line correspond to an unordered initial state with random initialization of the spins.

C. Energy histograms

We generate samples of ϵ from $N_{\text{MC}} = 10^5$ cycles for $T = 1\, J/k_B$ and $T = 2.4\, J/k_B$, with resulting histograms shown in Fig. 3. For $T = 1\, J/k_B$ we see that the distribution has a mean and variance of $\langle \epsilon \rangle \approx -2\, J$ and $\sigma(\epsilon)^2 \approx 5.91 \cdot 10^{-5}\, J$, with more than 80 % of the samples are drawn from microstates consisting of aligned spins where $\epsilon = -2\, J$. We notice that there are no samples in which $\epsilon = -1.99$, which would correspond to a single spin having the opposite orientation from the others. From equation (21) we see that this is due to flipping a single spin leads to the largest possible value of $\Delta E = 8\, J$, rendering configurations with a single anti-aligned spin very improbable.

For $T = 2.4\, J/k_B$, we see in the right panel of Fig. 3 that the energy of the system is distributed over a larger range, with $\langle \epsilon \rangle \approx -1.24\, J$ and $\sigma(\epsilon)^2 \approx 2.03 \cdot 10^{-2}\, J$. We see that there are no energy values around the mean that are inaccessible, compared to the low-temperature distribution in the left panel.

D. Phase transition

Using $N_{\text{MC}} = 10^5$ and $N_{\text{eq}} = 1.5 \cdot 10^4$, the estimated value of C_V and χ are plotted for $T \in [2, 2.5]\, J/k_B$ in

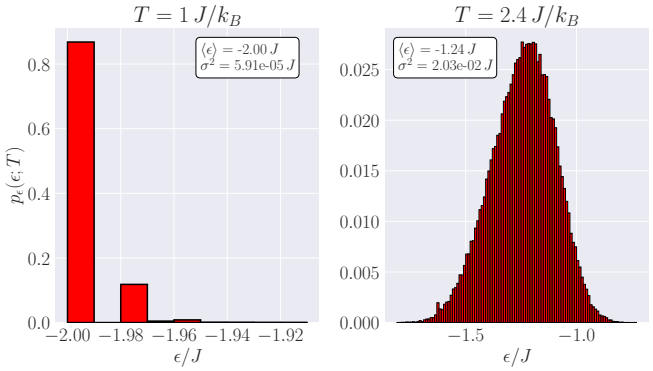

FIG. 3. Estimates of the probability distribution $p_e(\epsilon; T)$ for $T = 1\, J/k_B$ and $T = 2.4$. For $T = 1\, J/k_B$ the expectation value is $\langle \epsilon \rangle = -2.00\, J$ with variance $\sigma^2 = 5.91 \cdot 10^{-5}$, while for $T = 2.4$ the expectation value is $\langle \epsilon \rangle = -1.24\, J$ with variance $\sigma^2 = 2.03 \cdot 10^{-2}$.

the left and right panel of Fig. 4, respectively. We see a clear indication of a phase transition taking place, as both quantities shows diverging behavior near $T \sim 2.3\, J/k_B$. Since C_V is expected to diverge logarithmically, the maximum values differ little as we increase lattice size, compared to the maximum values we see for χ. With large variations of χ near the critical temperature, with respect to both lattice size and temperature, small statistical fluctuations can have a great impact on the predicted values of $T_C(L)$. To extract estimates of $T_C(L)$ we will therefore consider the heat capacity only in further investigations.

We estimate C_V for $T \in [2.25, 2.35]\, J/k_B$, with a spacing of $\Delta T = 10^{-3}$. To reduce the uncertainty of the measured averages, we now run $N_{\text{MC}} = 10^6$ cycles for each temperature value, using $N_{\text{eq}} = 1.5 \cdot 10^4$ still. The result is shown in Fig. 5, where dots represent the measured value of C_V for individual lattice sizes at each temperature, and the dashed lines represent the resulting fit from a cubic spline. The maximum points of the fitted function for the different lattice sizes is shown in the figure. It is also worth noticing the increase in variance of the estimates heat capacities as the lattice size increase.

Using the estimated values of $T_C(L)$, we perform linear regression with respect to inverse lattice sizes, and estimate approximate values for a and $T_C(L = \infty)$ from Eq. (15). The result of the linear regression is shown in Fig. 6, with the individual estimates of $T_C(L)$ included in the figure. The points corresponding to the lattice of size $L = \infty$ is also shown in the figure. We emphasize that the negative values on the x-axis in Fig. 6 is un-physical, and is only included to better see the estimated value of the critical temperature. The linear regression resulted in a slope of $a = 0.888$ and an intercept of $T_C(L = \infty) = 2.2651\, J/k_B$.

In table II we present the estimated values of the critical temperatures. The second column shows the estimated value of $T_C(L)$ from the maximum value of the fitted heat capacity. The critical temperature at different

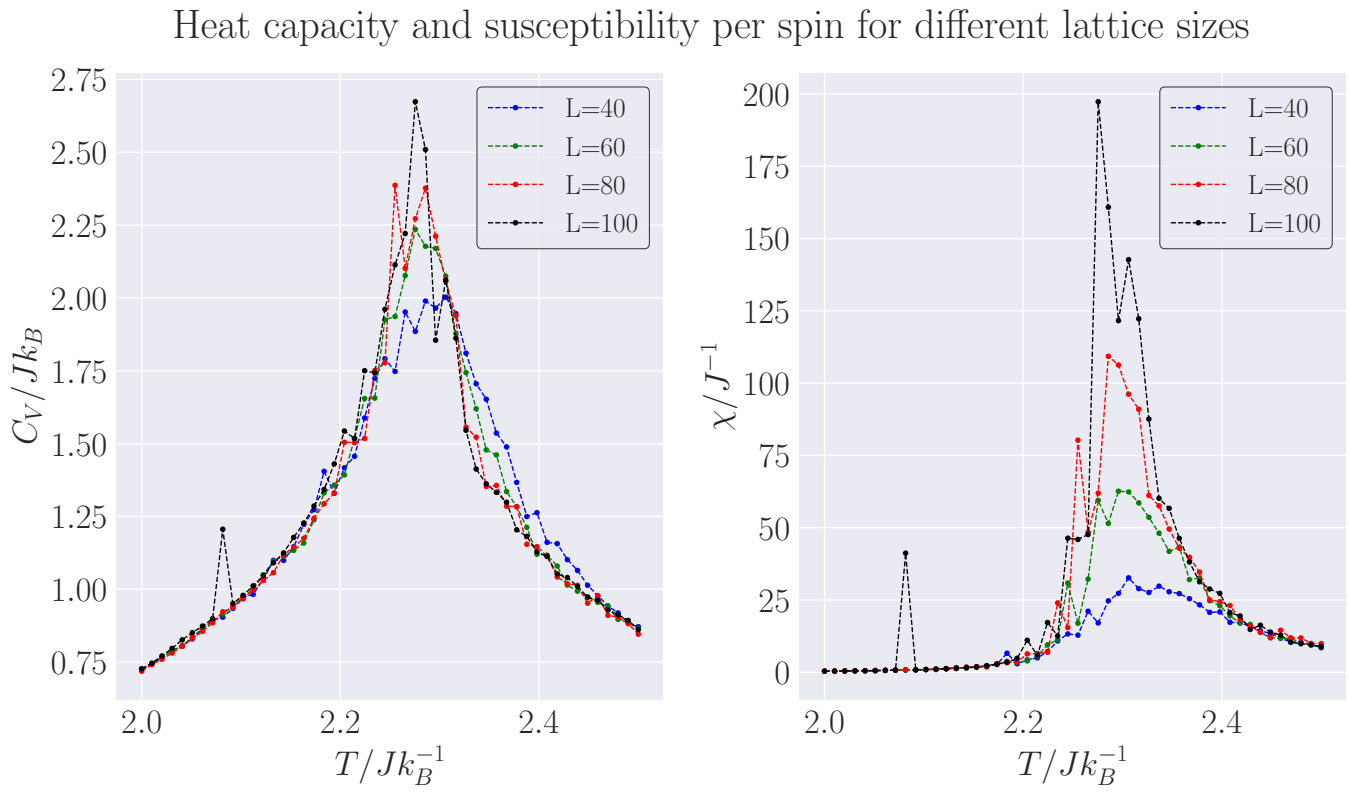

FIG. 4. Heat capacity C_V and magnetic susceptibility χ for lattices of different sizes $L \in \{40, 60, 80, 100\}$ for temperatures $T \in [2.0, 2.5]\, J/k_B$. In both panels we see clear indications of the power rule behavior these properties exhibit around their critical temperatures.

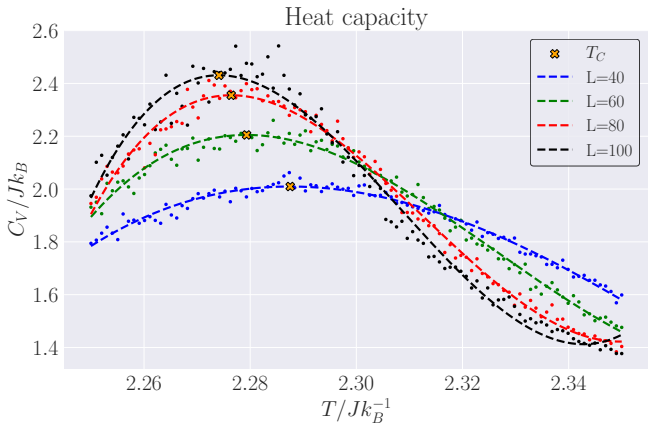

FIG. 5. Close up analysis for the heat capacity C_V for $T \in [2.25, 2.35]$ with maximum points estimated from an interpolation of the data points for each lattice size. These are shown as orange markers in the plot.

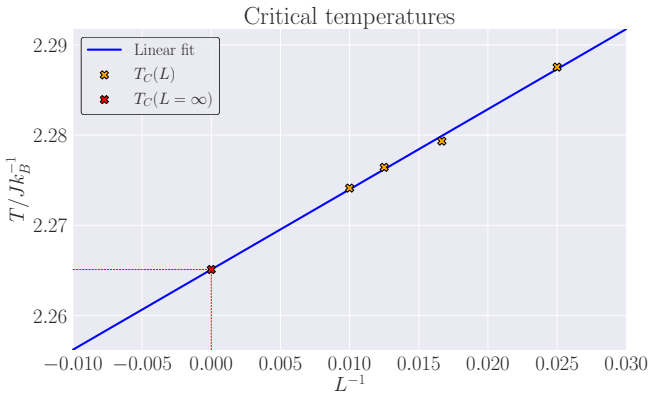

FIG. 6. Linear fit of the critical temperatures. The fit is made from the orange markers in the plot, as a function of the inverse lattice size. The critical temperature for an infinite lattice is found as the intercept of this linear fit and is marked with red in the plot.

lattice sizes according to the linear regression is shown in the third column. In the fourth column we have included the mean squared error (MSE) between the heat capacity data and the fit. Uncertainties related to errors like these were not accounted for when performing linear regression. The last row represents the infinite size lattice.

The discrepancy between our estimate of $T_C(L = \infty)$ and the true value is thus $\Delta T_C(L = \infty) \approx 4.1 \cdot 10^{-3}\, J/k_B$. In section VI we will discuss more in detail the validity of our results, with a particular emphasis on how to improve some of the results we have obtained, as well as some limitations of our methods in general.

L	T_c^{Cv} $[J/k_B]$	T_c^{linreg} $[J/k_B]$	MSE(C_V/Jk_B)
40	2.2875	2.2873	0.0004
60	2.2793	2.2799	0.0008
80	2.2764	2.2762	0.0011
100	2.2741	2.2740	0.0031
∞		2.2651	

TABLE II. Critical temperatures for different lattice sizes found both from curve fit and linear regression. $T_C(L = \infty)$ is estimated from linear regression only.

VI. DISCUSSION

A. Limitations of the Metropolis algorithm

One important limitations of our methods in general is that the Metropolis algorithm is not very efficient close to the critical temperature [1]. Cluster algorithms such as Wolff and Swendsen-Wang are much more efficient in simulating properties near the critical temperature. With this in mind, we limit the following discussions to improvements that can be done on our own implementations, with less emphasis on how to accurately determine the critical temperatures.

B. Sample sizes and equilibration

When we estimated the number of equilibration cycles, we did not account for other lattice sizes than $L = 20$. For the lattice sizes we used to determine critical temperatures, a higher number of cycles could be required to properly equilibrate the system. In Fig. 5 we see that there are large variations in C_V at different temperatures, and from the last column in table II we see that the variance increases for larger lattice sizes. One major drawback of our method is that we have only sampled averages at each temperature from a single MC simulation. To obtain results with more statistical significance an obvious choice is to perform repeated MC simulations, add these individual averages to obtain some final estimates of average quantities. An alternative approach which requires less additional computations would be to implement dynamical values of N_{MC} and N_{eq}, where we increase the number of cycles for larger lattices. Despite yielding less rigorous results in a statistical sense, it would reduce the uncertainties to some extent.

C. Estimating critical temperatures from curve fitting

When we estimate the critical temperature from the heat capacities, fitting the C_V data with cubic splines is arguable an approach with room for improvement. For $L = 100$ this is particularly evident, as there are some temperature regimes where the C_V data is almost consistently lower or higher than the fit. In Fig. 5 we see examples of this for $T \sim 2.31\, J/k_B$, where the data points lie below the spline, and for $T \sim 2.33\, J/k_B$ where the data points lie above it. A more careful consideration of how we perform the fit should therefore have been taken into account. If samples from multiple simulations had been used, as mentioned in the previous subsection, a natural way of approaching this would be to weight the fit at different temperatures according to the variance of the individual simulations.

This leads us to the linear regression, which was also performed without taking any statistical weights into account. It's evident from Fig. 5 that there is less variance in the measured C_V for $L = 40$ compared to $L = 100$. For the latter lattice size, we also see a large spread in the measured heat capacities near the critical temperature. This raises some concerns, as it implies that we have significant uncertainties in our estimates of the critical temperatures, particularly for larger lattice sizes. The linear regression should therefore have been adjusted so that it emphasizes less the critical temperature estimates obtained from the larger lattice sizes.

VII. CONCLUSION

In conclusion, we have simulated a 2D Ising model with no external magnetic field, by performing Monte Carlo simulation with the Metropolis algorithm. The model reproduces the expected existence of phase transitions near a critical temperature. We estimate the critical temperatures for four different lattice sizes, and use these values to obtain an estimate of the analytical value of the critical temperature for the 2D Ising model of infinite size. Our approximation reads $T_C(L = \infty) \approx 2.2651\, J/k_B$, which compared to the analytical expression $T_C(L = \infty) \approx 2.2692\, J/k_B$ is a fairly decent result, but slightly too low. With an improved algorithm better suited for critical temperatures (see section VI A), and/or a more thorough analysis, as discussed in sections VI B and VI C, the approximation of critical temperatures, and the efficiency of which, would probably be improved greatly. Our results do however lack a proper treatment of uncertainties. Although errors and model validity are discussed, without a proper treatment of the uncertainties we may only conclude that our obtained results are comparable estimates to the true analytical value.

VIII. ACKNOWLEDGEMENTS

We would like to offer our most sincere gratitude towards the tarmac in Blinderveien for its high bulk modulus, and the fragility of the human body. This work could not have been done without their combined support.

Appendix A: Analytical results

To derive the analytical expression for the (2×2) Ising model, we consider the number of spins with $+1$, and compute the energy, magnetization and degeneracy of the system for each of these. The resulting values are given in table III. For all positive or all negative spins, the energy of the system is $E = -8J$. For $N_\uparrow = 2$ there the only configuration yielding a non-negative energy is when the spins on the diagonal have the same orientation. In that case, we have $E = +8J$. Otherwise, the remaining configurations all have $E = 0$. The partition

$N_\uparrow$	$E(s)$	$M(s)$	Degeneracy
4	$-8\,\mathrm{J}$	4	1
3	0	2	4
2	$8\,\mathrm{J}$	0	2
2	0	0	4
1	0	-2	4
0	$-8\,\mathrm{J}$	-4	1

TABLE III. Analytical solutions to the (2×2) Ising model, where features of the system is tabulated as a function of the number of spins pointing up (being $+1$): $N_\uparrow$.

function can now be calculated with Eq. (4), using the degeneracy associated with the three possible energy values from table III,

$$Z = 12 + 2e^{-8\beta J} + 2e^{8\beta J} = 12 + 4\cosh(8\beta J). \tag{A1}$$

Using Eq. (5), we get the following analytical expectation values for the lattice,

$$\langle \epsilon \rangle = \sum_\nu \epsilon(\nu) \frac{1}{Z} e^{-\beta E(\nu)} = -\frac{8J}{Z} \sinh(8\beta J), \tag{A2}$$

$$\langle \epsilon^2 \rangle = \sum_\nu \epsilon(\nu)^2 \frac{1}{Z} e^{-\beta E(\nu)} = \frac{16J^2}{Z} \cosh(8\beta J), \tag{A3}$$

$$\langle |m| \rangle = \sum_\nu |m(\nu)| \frac{1}{Z} e^{-\beta E(\nu)} = \frac{2}{Z}\left(2 + e^{8\beta J}\right), \tag{A4}$$

$$\langle m^2 \rangle = \sum_\nu m(\nu)^2 \frac{1}{Z} e^{-\beta E(\nu)} = \frac{2}{Z}\left(1 + e^{8\beta J}\right). \tag{A5}$$

The resulting expressions for C_V and χ are thus

$$\begin{aligned} C_V &= \frac{\beta}{NT}\left(\langle E^2 \rangle - \langle E \rangle^2\right) \\ &= \frac{64\beta J^2}{ZT}\left[\cosh(8\beta J) - \frac{4}{Z}\sinh^2(8\beta J)\right], \end{aligned} \tag{A6}$$

$$\begin{aligned} \chi &= \frac{\beta}{N}\left(\langle M^2 \rangle - \langle M \rangle^2\right) \\ &= \frac{8\beta}{Z}\left[\left(1 + e^{8\beta J}\right) - \frac{2}{Z}\left(2 + e^{8\beta J}\right)^2\right]. \end{aligned} \tag{A7}$$

Appendix B: Parallel

Figure 7 show the run times for a simulation of $N_{\mathrm{MC}} = 10^5$ Monte Carlo cycles, with $N_{\mathrm{eq}} = 1.5 \cdot 10^4$ equilibration cycles for 20 temperatures on the interval $T \in [2.0, 2.5]$ as function of the lattice size L, both using `OpenMP` parallelization and standard serial runs of our code. We clearly deduce from the figure that a parallelized code runs faster, especially when the lattice size increase. This is a result of the large number of computations required for large lattices at each temperature step. For $L = 80$ the ratio between the computation times of serial and parallel, t_s and t_p are approximately

$$\frac{t_s}{t_p} = \frac{582.82}{207.01} \approx 2.82, \tag{B1}$$

which is less than the ideal speedup factor of five. A proper estimation of the speedup factor would be obtained by plotting the ratio t_s/t_p as a function of lattice sizes, obtained from average computational times over several measurements[5].

FIG. 7. Duration as function of lattice size for running $N_{\mathrm{MC}} = 10^6$ Monte Carlo cycles with $N_{\mathrm{eq}} = 1.5 \cdot 10^4$ equilibration cycles for 20 temperatures on the interval $T \in [2.0, 2.5]$. The parallelization is done using 5 threads and is shown in blue in the plot, against the serial implementation in red.

[5] This was planned, but could not be executed properly, due to a human brain-memory leakage during parallelization of the project work.

[1] Hjort-Jensen, M. (2015). Computation physics, lecture notes fall 2015.

[2] Onsager, L. (1944). Crystal statistics. i. a two-dimensional model with an order-disorder transition. *Phys. Rev.*, 65:117–149.

[3] Swendsen, R. H. (2020). *An Introduction to Statistical Mechanics and Thermodynamics*. Oxford science publications. Oxford University Press.

[4] Yeomans, J. M. (1992). *Statistical mechanics of phase transitions*. Oxford science publications. Clarendon Press, Oxford.